



SYNTHESIS AND CHARACTERISATION OF DIELECTRIC COMPOSITES PRODUCED FROM GLYCINE AND ALKALINE NIOBATE-BASED CERAMICS

Henry E. Mgbemere¹ and Viktoriya Semeykina²

¹ Department of Metallurgical and Materials Engineering, University of Lagos, Akoka Lagos Nigeria. Email: hmgbemere@unilag.edu

² Institute of Advanced Ceramics, Hamburg University of Technology Hamburg Germany. Email: Viktoriya.semeykina@tuhh.de

<https://doi.org/10.30572/2018/kje/150106>

ABSTRACT

Glycine exhibits a little piezoelectric response when poled, while lead-free alkaline niobate-based ceramics show much higher responses. This research investigates the synthesis of a dielectric composite from a combination of glycine and (K_{0.45}Na_{0.51}Li_{0.04}) (Nb_{0.85}Ta_{0.1}Sb_{0.04}) O₃ (KNNLST) ceramics. The mixed oxide ceramics synthesis method was used to produce the ceramics, while glycine powder was commercially procured. The composition range of the shaped and heat-treated composites is from no ceramics to 100 wt.% ceramics content. X-ray diffraction (XRD), Scanning Electron Microscopy (SEM), dielectric studies, and hysteresis measurements were used to characterize the samples. The obtained phases transformed from the monoclinic phase in glycine to a two-phase orthorhombic-tetragonal phase in the ceramics. The samples' morphology revealed a dense microstructure with some cracks, large porosity, and smaller grain sizes. The dielectric properties showed increasing dielectric constant and loss values with increasing ceramics content, while the ac conductivity also increased with rising ceramics content. Improving the range of ceramics led to polarization hysteresis graphs indicating ferroelectricity in the samples. The properties of the composites show they can be used in electromechanical devices.

KEYWORDS: Glycine, Composites, KNNLST Ceramics, Amino acid, Dielectric.

Article information: This manuscript was handled by Abbas Al-Hdabi, Managing Editor.



This work is licensed under a [Creative Commons Attribution 4.0](https://creativecommons.org/licenses/by/4.0/) International License.

1. INTRODUCTION

Electromechanical devices are usually produced from ceramic and polymeric materials for specific applications. Ceramics like BaTiO₃ (Sahu et al., 2021) and KNN (Abdullah et al., 2021), as well as polymers like polyvinylidene difluoride (PVDF) (Genchi et al., 2016), are usually the materials of choice in the fabrication of these devices. Ceramics production usually requires very high operating temperatures, which increases the cost, while polymers are limited by their low piezoelectric responses.

Specific applications require that the electromechanical device be compatible with the human body. There are reports in the literature that some amino acids, such as Glycine, exhibit piezoelectric responses (Guerin et al., 2018 and Bishara et al., 2020). It exists in three crystallographic forms: α , β , and γ . The first two forms are centrosymmetric with a $P2_1/c$ space group, while γ -glycine is non-centrosymmetric with a $P3_1$ space group. The difference between these glycine forms is in the angles their chemical bonds form between the zwitterions. Theoretical calculations have been used to predict that amino acids like glycine, hydroxyproline, and lysine are non-centrosymmetric and exhibit high piezoelectric response (Guerin et al., 2019). Di-phenylalanine was simulated to have the highest piezo-response because external electric fields easily influence it in aqueous solutions.

When exposed to different fluids, glycine undergoes polymorphic transitions, indicating their stability level where $\beta < \alpha < \gamma$ (Boldyreva et al., 2003a). This polymorphism has been investigated using 3D electron diffraction, showing that the α and β forms are thermodynamically unstable while the γ form is stable (Broadhurst et al., 2020). However, based only on kinetic considerations, the α -form is believed to be the most stable form of glycine. Although α -glycine is centrosymmetric, it exhibits pyro and piezoelectric response due to polar near-surface structures resulting from the interactions with solvent and impurities. Glycine crystals are brittle, and when the α -phase is compressed, the dipole moment is created in the lattice, thereby increasing the net polarization.

NaCl has been used to grow γ -glycine, which was characterized using carbon, hydrogen, and nitrogen (CHN) analysis, infrared spectroscopy, XRD, and differential scanning calorimetry (DSC) (Bhat and Dharmaprakash, 2002). Nanocrystals of β -glycine and L-alanine have been used to produce sensors that could detect ultralow mechanical pressure (Bishara et al., 2020). The growth of amino acids is affected by the quantity and type of additives, like oxalic acid, NaCl, ethanol, etc., during their synthesis (Hrkovac et al., 2011).

Supramolecular packing of the atoms has been shown to enhance the control of piezoelectricity in amino acids, but piezoelectric responses between $0.1\text{--}10\text{ pmV}^{-1}$ tend to limit the application (Guerin et al., 2018). Combining the piezoelectric response of amino acids with materials with high piezo-response to form composites is necessary. Biocompatible and flexible piezoelectric stress sensor from γ -glycine micro-crystals embedded in polydimethylsiloxane (PDMS) gave an average voltage of 250 mV, current density of $0.010\text{ }\mu\text{A}/\text{cm}^2$ and a power density of $2.5\text{ nW}/\text{cm}^2$ (Hosseini et al., 2018). A biodegradable pressure sensor from β -glycine and chitosan sandwiched between Mg electrodes reached a sensitivity of $\sim 1.42\text{ mV}$ when pressures between 5 and 25 kPa were applied (Hosseini and Dahiya, 2020). Glycine molecules embedded in the chitosan matrix produced pressure sensors in the $0\text{--}40\text{ kPa}$ range and output voltages of up to 180 mV, resulting in a sensitivity of approx. 4.7 mV kPa^{-1} (Hosseini et al., 2020). The possibility of totally removing lead-based piezoelectric materials and replacing them with low-cost, high-performance biomolecular crystals has been discussed with the hypothesis that wafer-level biomolecules with a similar piezo response as PZT can be produced in the future (Guerin, 2022). Lead-free ceramics based on $(\text{K}_{0.45}\text{Na}_{0.51}\text{Li}_{0.04})(\text{Nb}_{0.85}\text{Ta}_{0.1}\text{Sb}_{0.04})\text{O}_3$ ceramics (abbreviated as KNNLST) have been made and mixed with glycine to form a composite. This research aims to produce composites that can be biocompatible the human body, has adequate piezoelectric response for possible use in electromechanical devices. Since amino acids are compatible with the body, it will lead to the development of very important biocompatible devices.

2. MATERIALS AND METHODS

2.1. Ceramics Synthesis

Raw powders of Na_2CO_3 , Li_2CO_3 , K_2CO_3 , (99+%), Nb_2O_5 , Ta_2O_5 (99.9%) (Chempur Feinchemikalien und Forschungs GmbH, Karlsruhe, Germany), and Sb_2O_3 (99.9%) (Alfa Aesar GmbH Kandel, Germany) were used for the ceramic synthesis without modification. The powders were dosed in their stoichiometric amounts and attrition milled for 2 h using 3 mm diameter ZrO_2 balls at a speed of 500 rpm and ethanol as solvent. Particle size analysis was carried out on the powder to determine its particle size after milling. The solvent was removed from the solution using a solvent extractor. The powder was calcined in a tube furnace at a heating rate of $3^\circ\text{C}/\text{min}$ to 850°C for 4 h and a cooling rate of $10^\circ\text{C}/\text{min}$. The milling process was repeated using the same parameters to ensure the homogeneity of the powder.

2.2. Composite Synthesis

Glycine (Glentham Life Sciences, Corsham, United Kingdom) was also used without modification. The idea behind this experimental setup is to determine how the properties will vary in the composites with changes in composition. The knowledge gathered from extensive work on lead-free ceramics also helped in the choice of some of the parameters used. The compositions of the composites are as follows: 0, 20, 40, 50, 60, 80, and 100 wt.% of the ceramics. The correct amounts of the amino acids were dissolved in deionized water, and the resulting solution was placed in a magnetic stirrer for 90 min at 60°C until a clear solution was obtained. The KNNLST ceramic is weighed, added to the solution, and stirred for another 90 min at 70°C. Ethanol was then added to the solution to help precipitate the particles. The solution was then placed in a centrifuge at 500 rpm for 5 min, and the resulting clear solution was decanted. The powder is then dried at room temperature for 72 h. The composite powder was initially pressed using uniaxial pressing at 10 KN for 30 s and a cold isostatic press at 500 MPa for 2 min. The pressed samples were then put inside an oven whose temperature was gradually increased from 100°C to 150°C for 48 h.

2.3. Composite Characterization

The density value of the samples was determined geometrically by measuring the mass and volume of the samples; a minimum of 5 samples was used for each composition. The X-ray diffraction analysis of the samples was carried out with a Bruker D8 Discover diffractometer with $\text{CuK}\alpha$ anode ($\lambda = 1.5406 \text{ \AA}$) at a voltage of 40 kV and 40 mA. The measurement was made in Grazing incidence diffraction mode (GID) with a source fixed angle of 5°, scanning speed of 3 s with an increment of 0.01° and measurement range from 10 to 60°. The samples for ferroelectric characterization were poled at fields between 1 to 3 kV/mm for 5 min, depending on the composition. The dielectric measurements were carried out using an LCR meter (HP 4284 USA). Silver paint was used to coat the samples in preparation for the measurement. Metallic wires were attached to the samples and measured from 20 Hz to 1 MHz.

The samples for microstructural characterization were carried out using a Scanning Electron Microscope (Zeiss Supra VP 55, Jena, Germany). Silver paints were applied to the sides of the sample to ensure adequate conductivity. The sample was inserted into the chamber, and enough vacuum was created before image acquisition using secondary electron detection mode. The samples for polarization hysteresis were coated on both sides and inserted into silicon oil to reduce the incidence of dielectric breakdown. A Sawyer-Tower circuit connected to a high-voltage generator was used for the measurement. The extent of polarization in the samples was

calculated by multiplying the capacitance with the obtained voltage and dividing it by the cross-sectional area of the sample.

3. RESULTS AND DISCUSSION

3.1. Density

The obtained density values for the glycine-KNNLST composites before and after heat treating the samples are shown in Fig. 1. The graph shows that the density before heat treatment is slightly higher than after heat treatment because moisture is lost during the heat treatment process. For the glycine sample, the density is 1.478 g/cm^3 , and as the content of KNNLST ceramics increases, the increase in density values is nearly linear and reaches a maximum value of $2.73 \pm 0.08 \text{ g/cm}^3$ at 80 wt. %. The KNNLST ceramics were sintered, so there is no need for before and after heat treatment, and a density value of $4.67 \pm 0.08 \text{ g/cm}^3$ was obtained. Compared to the density of the composite with 80 wt.% ceramics content, the density of the ceramics is ~ 1.7 times more.

The increase in density values of the composites with increasing amounts of KNNLST ceramics is because of the higher density of KNNLST ceramics compared to the glycine. However, these composite density values should be higher because of the less-than-optimal heat treatment process. This means many open pores could not be closed effectively, and the cracks introduced during pressing could also not be removed.

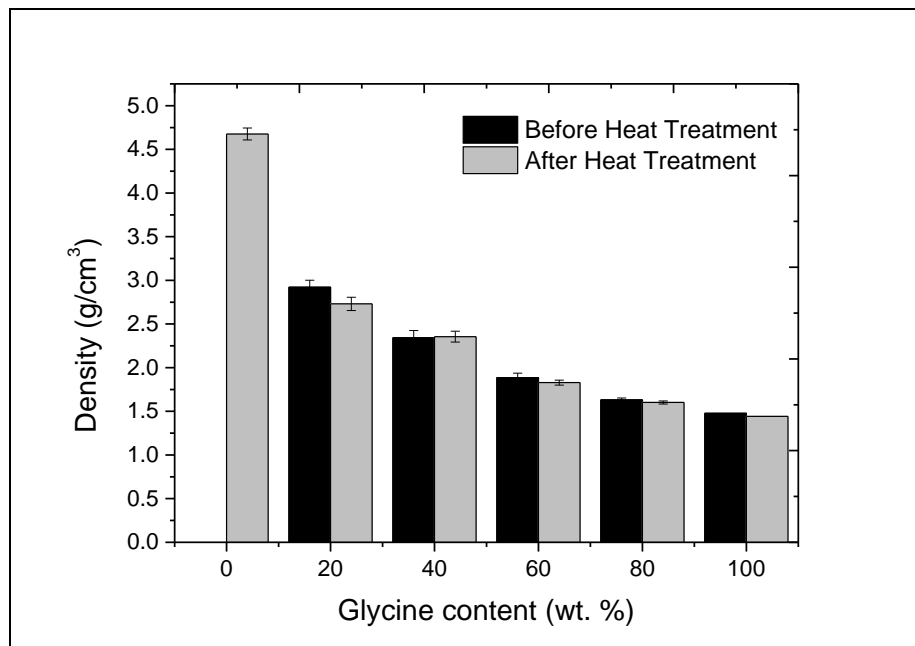


Fig. 1. Bulk Density value of the glycine – KNNLST ceramic composites obtained at room temperature.

3.2. X-ray diffraction

The plot of the X-ray diffraction patterns for glycine-KNNLST composites is shown in Fig. 2. The diffraction pattern for glycine shows that crystalline but achiral α -glycine molecules are present. The crystal structure is evaluated to be monoclinic with a $P2_1/c$ space group, and the crystallographic indices are indicated. It is centrosymmetric but exhibits piezoelectric properties when mixed with piezoelectric materials (Boldyreva et al., 2003b). Peak matching with the crystallographic database reveals that the γ -glycine fits the diffraction patterns of glycine in the composites. On adding 20 wt.% of KNNLST ceramics, the diffraction patterns started transforming to form a combination of both diffraction patterns for glycine and KNNLST. When the KNNLST content increased to 80 wt.%, the diffraction pattern for the ceramics became dominant, although a few peaks from glycine could still be observed. It is believed that the introduction of KNNLST changed the angle of the chemical bond in the composites.

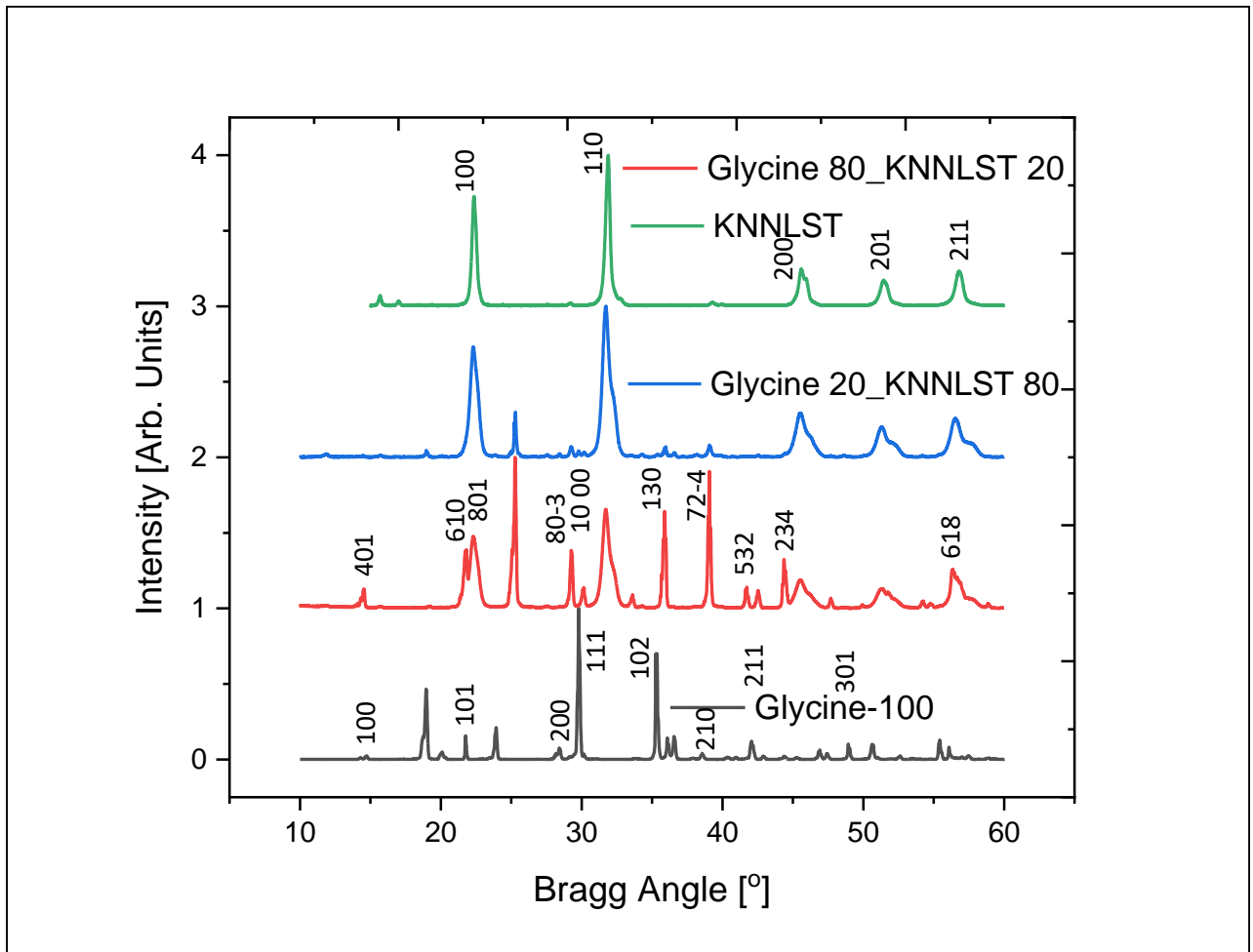


Fig. 2. Graph of X-ray diffraction patterns for the glycine-KNNLST composites.

3.3. Scanning Electron Microscope

The micrographs of the glycine-KNNLST composites are shown in Fig. 3. The grain boundaries, voids, cracks, and grains have been labelled in the diagrams. The morphology of pure glycine shows that it is crystalline with grains and their boundaries, consistent with the X-ray diffraction observation. The mean intercept length method was used to estimate the average grain size of the samples. Huge particle sizes of most grains are observed, with some grains as long as 20 μm and a few small grains. Some porosity in the samples is observed, especially around the grain boundaries. Microcracks could be seen inside the sample, and also, in some large grains, there appear to be tiny grains when the KNNLST ceramic content in the composite is 20 wt. %, the sample's surface becomes highly porous with some more than 10 μm in diameter pores. The sample is still crystalline with clear grain boundaries; most grains are still significant with more than 50 μm sizes. There are also small grains on the surfaces of the large grains. Some grains are rod-like, and cracks can be observed on the sample surface. Rod-like grains and cracks could also be observed on the sample surface. When the content of KNNLST ceramics present is 40 wt.%, large grains of about 30 μm size are observed. However, the level of porosity is slightly reduced with dimensions of approx. 10 μm , and in some cases, they are interconnected. The volume of grains with sub-micron size increases, although some sample sections appear amorphous. Rod-like grains, as well as cracks, are also observed on the sample surface. The cracks are more prominent when the content of the ceramics increases. As its content increases, the cracks become more pronounced due to the increased strain due to differences in the physical properties of both materials and the pressure applied. As the ceramics content in the composite increases to 60 wt.%, submicron-sized grains become more dominant, although large pores are present in some sections of the sample. The size of the large grains is about 1 μm , and the rod-like nature of the grains becomes more pronounced. Further increasing the content of the ceramic to 80 wt. % increases the volume of the submicron-sized grains with some porosity in some sections of the micrograph. More rod-like grains are present in the sample, with some interconnecting pores and cracks on the sample. The morphology of the KNNLST ceramics shows the usual quasi-cubic morphology with grain sizes mostly < 1 μm . The reason why the grain size is mainly in the sub-micron range can be traced to the sample preparation method. The dense nature of the structure is reflected in the relatively high-density value, which is ~ 97% of its theoretical density. Based on the microstructures investigated, the composite with composition 40% glycine and 60 wt. % KNNLST has very small particles sizes, low porosity and few cracks. When all the measured properties are considered, it is therefore believed to have the best properties.

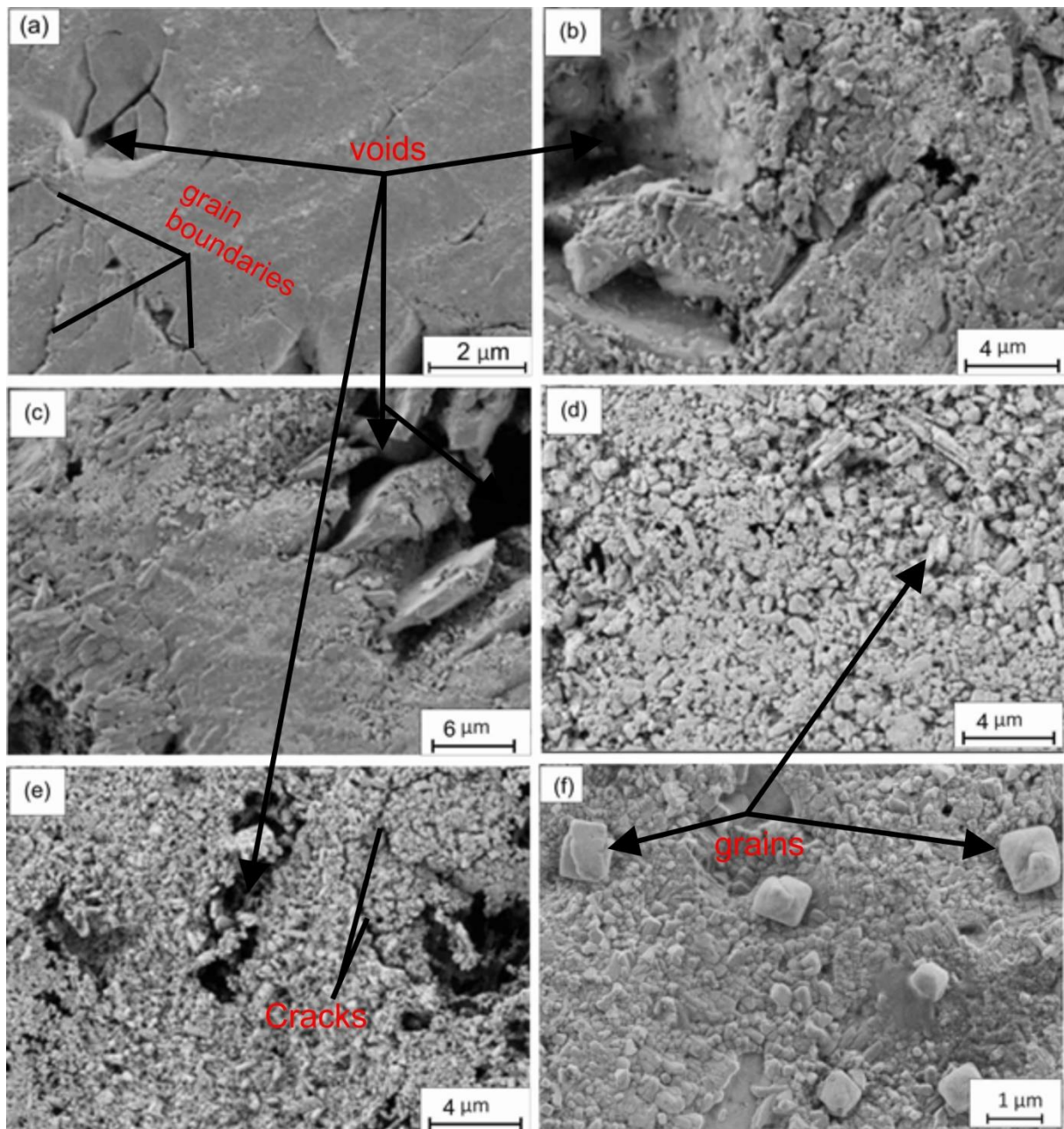


Fig. 3. Scanning Electron Microscope images of (a) Glycine (b) Gly 80-KNNLST 20 (c) Gly 60-KNNLST 40 (d) Gly 40-KNNLST 60 (e) Gly 20-KNNLST 80 composites.

3.4. Dielectric properties

The dielectric constant values for the glycine-KNNLST composites are shown in Fig. 4. The dielectric constant value for glycine is 9 at a frequency of 20 Hz and remains almost constant up to 1 MHz. As the KNNLST ceramics content in the composite is 20 wt.%, the dielectric constant steady increases to 30 at 20 Hz and slightly decreases to 10 at 1 MHz. When the content increases to 40 wt.%, the dielectric constant increases to 42 and gradually decreases to around 15 at 1 MHz. The higher the range of the KNNLST ceramics, the higher the obtained dielectric constant value. When the content of the ceramic has increased to 80 wt.%, the dielectric

constant value rises to 1000 at 20 Hz and gradually decreases to slightly below 100 at 1 MHz. The dielectric constant of the KNNLST ceramics is relatively stable over the range of frequencies measured. A value of 1200 was obtained at 20 Hz and gradually slightly decreased to below 1000 at 1 MHz.

The dielectric loss values for the glycine-KNNLST composite are shown in [Fig.4b](#). Relatively high loss values were obtained for the samples at lower frequencies, which gradually decreased at higher frequencies. At 20 Hz, the loss in glycine is 0.3, and it gradually decreases to less than 0.01 at 1 MHz, with 20 wt.% ceramics content, the loss tangent at 20 Hz is 1, slowly falling to 0.1 at 1 MHz, with 40 wt.% KNNLST in the composite, the loss tangent increases to 2 at 20 Hz and progressively decreases to approx. 0.1 at 1 MHz. The increments in ceramics content to 60 and 80 wt.% yielded similar results where the dielectric loss was 3 at 20 Hz and gradually decreased to 0.2 at 1 MHz. The dielectric loss in the KNNLST ceramics showed that between 20 Hz and 1 MHz, the dielectric loss values were at approximately 0.1. and discontinuities in values were also observed to occur at specific frequencies. The discontinuities observed in the dielectric constant and dielectric loss values may be related to the resonances in the KNNLST ceramics.

The dielectric loss is the energy loss associated with the applied electric field being ahead of the polarization shift ([Rayssi et al., 2018](#)). It is affected by sample composition, preparation method, porosity, etc. It originates from the migration of space charges (interfacial polarization contribution), direct current (DC) conduction, and movement of the molecular dipoles (dipole loss) ([Rayssi et al., 2018](#)). Dielectric loss due to conduction, where the flow of charge in a substituting electromagnetic field as polarization switches direction through the composite, leads to energy dissipation was observed. As the polarization delays the applied field, an interaction occurs between the field and the dielectric's polarization, which causes material heating. The dielectric and ferroelectric properties show improved properties similar to reports in the literature for ceramics with similar compositions ([Mgbemere et al., 2012](#)).

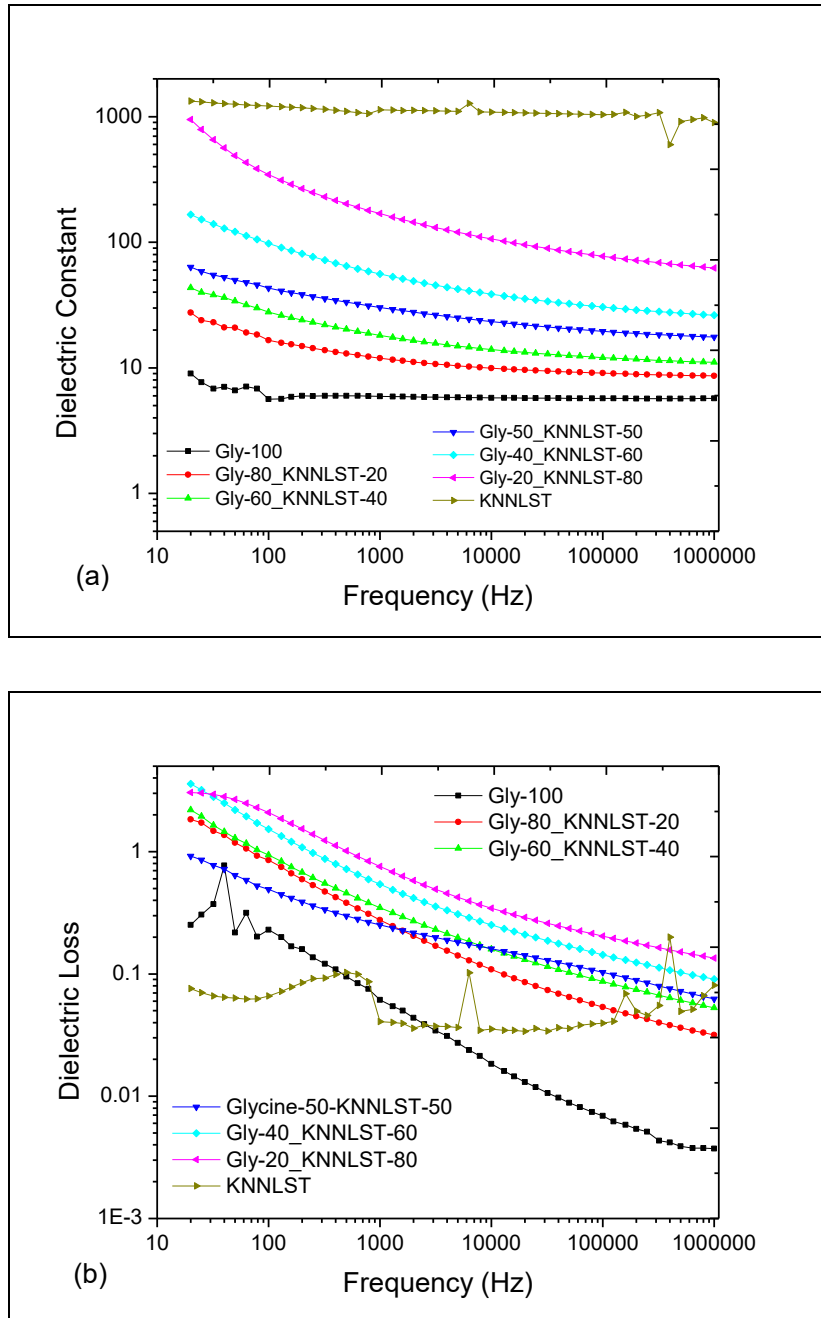


Fig. 4. Plots of (a) dielectric constant and (b) dielectric loss for glycine-KNNLST ceramic composites measured at room temperature.

3.5. Conductivity

The plot of conductivity as a function of frequency for glycine-KNNLST composites is shown in Fig. 5. Glycine has the lowest conductivity values in the range of frequency measured. At 20 Hz, the value is 2×10^{-9} S/m and almost linearly increases to 8×10^{-7} S/m at 1 MHz. When 20 wt.% of KNNLST ceramics is added to glycine, the conductivity value increases to 5×10^{-8} S/m and linearly increases to 5×10^{-6} S/m. The introduction of more KNNLST ceramics resulted in the same pattern of increasing conductivity values such that at 80 wt.% of KNNLST ceramics, the conductivity has increased to 3×10^{-6} S/m at 20 Hz, which increases to 2×10^{-4} S/m at 1

MHz. KNNLST ceramics has an even poorer conductivity value with 1×10^{-7} S/m at 20Hz, which increased to 3×10^{-3} S/m at 1 MHz.

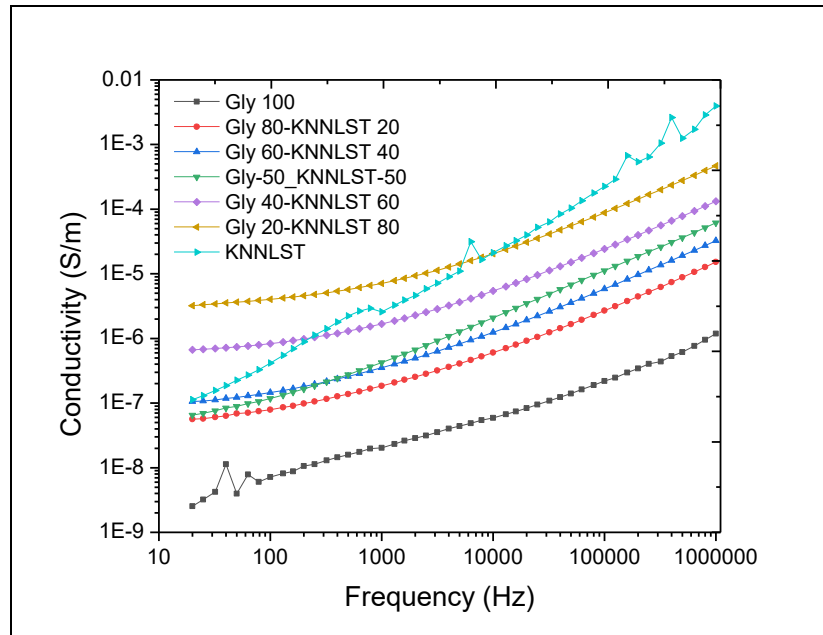


Fig. 5. A graph of conductivity for glycine-KNNLST composite measured at room temperature.

3.6. Polarization Hysteresis

The graph of polarization as a function of the applied electric field for the glycine-KNNLST composite is shown in Fig. 6. The hysteresis curves show that unusually high hysteresis loops bigger than those of KNNLST ceramics were obtained for a few samples. The shape of the hysteresis loops was affected by factors such as dipole moments, domain switching, electric conductivity, equivalent field, and dielectric permittivity of the material. The egg-shaped hysteresis loops in this work are attributed mainly to electric conductivity, as evidenced by relatively high dielectric loss. The composites based on glycine-KNNLST exhibited some form of polarization hysteresis curves. Saturation polarization was not attained by applying a 2 kV/mm field. The presence of pores, cracks, and low-density values affected the polarization.

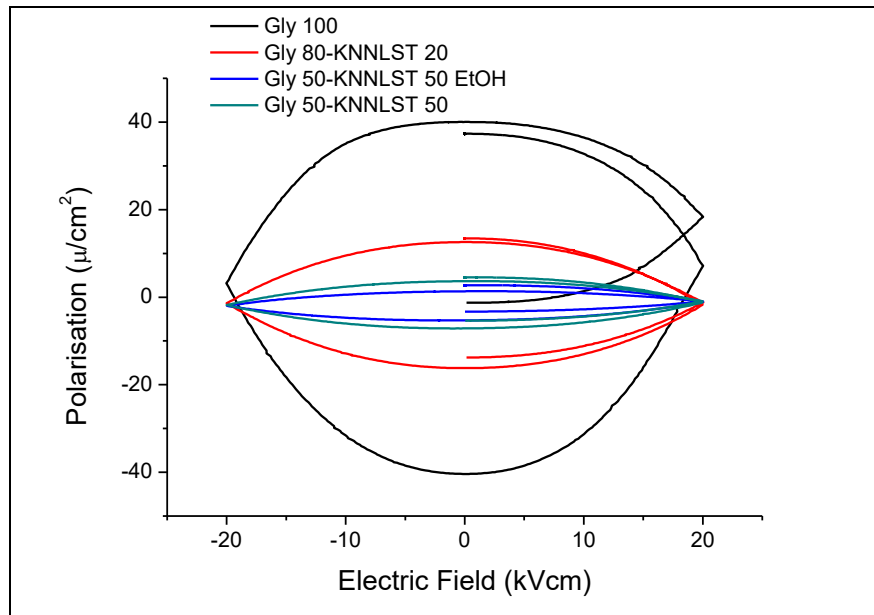


Fig. 6. A polarization plot as a function of electric field for glycine-KNNLST composite.

4. CONCLUSIONS

This research has investigated the properties obtained when glycine and KNNLST ceramics are used to form composites. As expected, the density results show that increasing the ceramic content led to increased density values of the composites. The maximum possible density values could not be obtained because the samples could not be sintered. The diffraction patterns revealed that α -glycine, which is crystalline, was obtained. As the amount of KNNLST ceramics increases, the diffraction pattern begins to transform until the dominant structure becomes that of the KNNLST ceramics. The morphology of the samples shows that glycine has huge grains. As the ceramics content increases, the particle size of the grains reduces with increasing porosity and cracks in the composite. The introduction of KNNLST ceramics to the glycine increased both the dielectric constant and the dielectric loss. The conductivity values of the samples also increased with rising ceramics content. The polarization experiment showed that huge hysteresis curves were obtained, indicating that factors outside the contribution of dipole moment were involved. The results show that the piezoelectric response of glycine has been improved with the addition of KNN ceramics.

5. ACKNOWLEDGEMENT

The authors acknowledge the help from Prof. G. A. Schneider, who made this research possible through funding from the German Research Foundation.

6. REFERENCES

- Abdullah, A. M., Sadaf, M. U. K., Tasnim, F., Vasquez, H., Lozano, K. & Uddin, M. J. (2021) Knn Based Piezo-Triboelectric Lead-Free Hybrid Energy Films. *Nano Energy*, 86, 1-43. <https://doi.org/10.1016/j.nanoen.2021.106133>.
- Bhat, M. N. & Dharmaprakash, S. M. (2002) Growth Of Nonlinear Optical Γ -Glycine crystals. *Journal of Crystal Growth*, 236, 376–380. [https://doi.org/10.1016/S0022-0248\(01\)02094-2](https://doi.org/10.1016/S0022-0248(01)02094-2)
- Bishara, H., Nagel, A., Levanon, M. & Berger, S. (2020) Amino Acids Nanocrystals for piezoelectric detection of ultra-low mechanical pressure. *Materials Science & Engineering C*, 108, 1-7. <https://doi.org/10.1016/j.msec.2019.110468>
- Boldyreva, E. V., Drebuschak, V. A., Drebuschak, T. N., Paukov, I. E., Kovalevskaya, Y. A. & Shutova, E. S. (2003a) Polymorphism of Glycine Thermodynamic aspects. Part II. Polymorphic transitions. *Journal of Thermal Analysis and Calorimetry*, 73, 419–428. <https://doi.org/10.1023/A:1025457524874>
- Boldyreva, E. (2021) Glycine: The Gift That Keeps On Giving. *Isr. J. Chem.*, 61, 828 – 850
- Broadhurst, E. T., Xu, H., Clabbers, M. T. B., Lightowler, M., Nudelman, F., Zou, X. & Parsons, S. (2020) Polymorph evolution during crystal growth studied by 3D electron diffraction. *IUCrJ*, 7, 5–9. <https://doi.org/10.1107/S2052252519016105>
- Genchi, G. G., Ceseracciu, L., Marino, A., Labardi, M., Marras, S., Pignatelli, F., Bruschini, L., Mattoli, V. & Ciofani, G. (2016) P(Vdf-Trfe)/BaTiO₃ Nanoparticle Composite Films Mediate Piezoelectric Stimulation and Promote Differentiation of SH-SY5Y Neuroblastoma Cells. *Adv. Healthcare Mater.*, 5, 1808–1820. <https://doi:10.1002/adhm.201600245>
- GUERIN, S. (2022) Getting the Lead Out: Biomolecular Crystals as Low-Cost, HighPerformance Piezoelectric Components. *Acc. Mater. Res.*, 3, 782–784. <https://doi.org/10.1021/accountsmr.2c00124>
- Guerin, S., Stapleton, A., Chovan, D., Mouras, R., Gleeson, M., Mckeown, C., Noor, M. R., Silien, C., Rhen, F. M. F., Kholkin, A. L., Liu, N., Soulimane, T., Tofail, S. A. M. & Thompson, D. (2018) Control of piezoelectricity in amino acids by supramolecular packing. *Nature Materials* 17, 180-188. <https://doi:10.1038/NMAT5045>
- GUERIN, S., TOFAIL, S. A. M. & THOMPSON, D. (2019) Organic piezoelectric materials: milestones and potential. *NPG Asia Materials* 10, 11, 1-5. <https://doi.org/10.1038/s41427-019-0110-5>

Hosseini, E. S. & Dahiya, R. (2020) Biodegradable Amino acid-based Pressure Sensor. IEEE, 1-4. <https://doi:10.1109/SENSORS47125.2020.9278878>.

Hosseini, E. S., Manjakkal, L. & Dahiya, R. (2018) Bio-organic Glycine based Flexible Piezoelectric Stress Sensor for Wound Monitoring. IEEE. 1-4 <https://doi:10.1109/ICSENS.2018.8589588>.

Hosseini, E. S., Manjakkal, L., Shakthivel, D. & Dahiya, R. (2020) Glycine–Chitosan-Based Flexible Biodegradable Piezoelectric Pressure Sensor. ACS Appl. Mater. Interfaces 12, 9008–9016. <https://doi.org/10.1021/acsami.9b21052>

Hrkovac, M., Kardum, J. P., Schuster, A. & Ulrich, J. (2011) Influence of Additives on Glycine Crystal Characteristics. Chem. Eng. Technol., 34, 611–618. <https://doi.org/10.1002/ceat.201000532>

Mgbemere, H. E., Herber, R.-P. & Schneider G. A. (2012) Effect of MnO₂ on the dielectric and piezoelectric properties of alkaline niobate based lead free piezoelectric ceramics. J. Eur. Ceram. Soc., 29, 1729-1733. <https://doi.org/10.1016/j.jeurceramsoc.2008.10.012>

Rayssi, C., El.Kossi, S., Dhahri, J. & Khirounib, K. (2018) Frequency and temperature-dependence of dielectric permittivity and electric modulus studies of the solid solution Ca_{0.85}Er_{0.1}Ti_{1-x}Co_{4x}/3O₃ (0 ≤ x ≤ 0.1). RSC Adv., 8, 17139–17150. <https://doi.org/10.1039/C8RA00794B>

Sahu, M., Hajra, S., Lee, K., Deepti, P. L., Mistewicz, K. & Kim, H. J. (2021) Piezoelectric Nanogenerator Based on Lead-Free Flexible PVDF-Barium Titanate Composite Films for Driving Low Power Electronics. Crystals, 11, 1-10. <https://doi.org/10.3390/cryst11020085>.